ADVANCED FUNCTIONAL MATERIALS
www.afm-journal.de

A Memristive Nanoparticle/Organic Hybrid Synapstor for Neuroinspired Computing

*Fabien Alibart, Stéphane Pleutin, Olivier Bichler, Christian Gamrat, Teresa Serrano-Gotarredona, Bernabe Linares-Barranco, and Dominique Vuillaume**

A large effort is devoted to the research of new computing paradigms associated with innovative nanotechnologies that should complement and/or propose alternative solutions to the classical Von Neumann/CMOS (complementary metal oxide semiconductor) association. Among various propositions, spiking neural network (SNN) seems a valid candidate. i) In terms of functions, SNN using relative spike timing for information coding are deemed to be the most effective at taking inspiration from the brain to allow fast and efficient processing of information for complex tasks in recognition or classification. ii) In terms of technology, SNN may be able to benefit the most from nanodevices because SNN architectures are intrinsically tolerant to defective devices and performance variability. Here, spike-timing-dependent plasticity (STDP), a basic and primordial learning function in the brain, is demonstrated with a new class of synapstor (synapse-transistor), called nanoparticle organic memory field-effect transistor (NOMFET). This learning function is obtained with a simple hybrid material made of the self-assembly of gold nanoparticles and organic semiconductor thin films. Beyond mimicking biological synapses, it is also demonstrated how the shape of the applied spikes can tailor the STDP learning function. Moreover, the experiments and modeling show that this synapstor is a memristive device. Finally, these synapstors are successfully coupled with a CMOS platform emulating the pre- and postsynaptic neurons, and a behavioral macromodel is developed on usual device simulator.

1. Introduction

Spike-timing dependent plasticity (STDP) is widely believed today to be one of the fundamental mechanisms of the unsupervised learning in biological neural networks. STDP in biological systems is a refinement of Hebb's learning rule.[1] Grant et al,[2] Markram et al,[3] Bi, and Poo[4] observed STDP in biological synapses. The principle of STDP is to tune the response of a synapse as a function of the pre- and post- synaptic neurons spiking activity - **Figure 1**a. Depending on the correlation or anti-correlation of the spiking events of the pre- and post-synaptic neurons, the synapse's weight is reinforced or depressed, respectively. The so-called "STDP function" or "STDP learning window" is defined as the relationship between the change in the synaptic weight or synaptic response versus the relative timing between the pre- and postsynaptic spikes (Figure 1b).[5] The implementation of STDP with nanodevices is strongly driven by a bio-inspired approach to enable local and unsupervised learning capability in large artificial SNN in an efficient and robust way. To this end, it is envisioned to use the nanodevices as synapses and to realize the neuron functionality with complementary metal oxide semiconductor (CMOS) technology. This approach is supported by the fact that the limiting integration factor is really the synapse density, as realistic applications could require as much as 10^3 to 10^4 synapses per neuron. Snider[6] proposed an implementation of STDP with nanodevices, where the synapses are realized with a crossbar of memristors[7] and the neurons with a "time-multiplexing CMOS" circuit. Using these two elements, it should be possible to reproduce exactly the "STDP learning window" of a biological synapse (Figure 1b). Linares-Barranco et al. simulated the implementation of the STDP function with memristive nanodevices.[8,9] Using a specific shape of the spikes and the nonlinearity of the memristor, they showed that the conductivity of the memristor can be tuned depending on the precise timing between the postsynaptic and presynaptic spikes. More interestingly, they showed that the shape of the STDP learning window can be tuned by changing the shape of the spike (Figure 1c). We have to emphasize that our aim is to be inspired by the behavior of a biological synapse for neural computation applications (and not to build a model system of the synapse), thus the important point is to reproduce qualitatively the STDP behavior, even if the spike signals applied to the synapstor are not close to the real biological spike.

Dr. F. Alibart, Dr. S. Pleutin, Dr. D. Vuillaume
Institute for Electronics Microelectronics and Nanotechnology (IEMN)
CNRS, University of Lille
BP60069, avenue Poincaré, F-59652cedex
Villeneuve d'Ascq, France
E-mail: dominique.vuillaume@iemn.univ-lille1.fr
O. Bichler, Dr. C. Gamrat
CEA, LIST/LCE (Advanced Computer technologies and Architectures), Bat. 528, F-91191, Gif-sur-Yvette, France
Prof. T. Serrano-Gotarredona, Prof. B. Linares-Barranco
Instituto de Microelectrónica de Sevilla (IMSE)
CNM-CSIC, Av. Americo Vespucio s/n, 41092 Sevilla, Spain

DOI: 10.1002/adfm.201101935

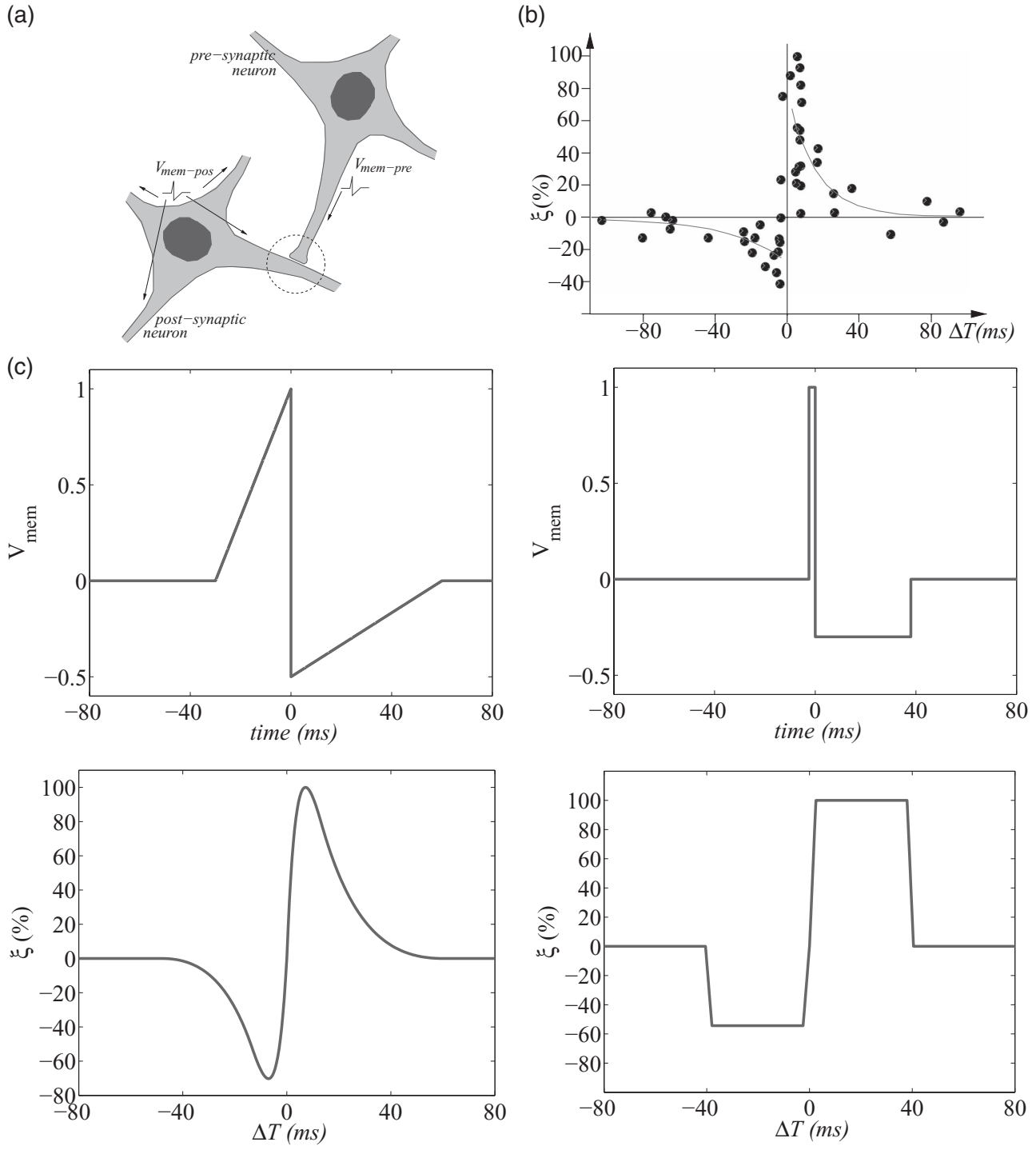

Figure 1. a) Illustration of a synapse connecting two neurons: the presynaptic and the postsynaptic neurons. Reproduced with permission.[9] b) STDP function, i.e., change in the synaptic weight versus spike timing interval, measured on a biological synapse. Reproduced with permission;[9] data from Bi and Poo.[4] c) Two shapes of spikes (left side) and the corresponding STDP functions (right side) calculated for a memristive device. Reproduced with permission.[9]

We recently demonstrated that the nanoparticle–organic memory field-effect transistor (NOMFET) is able to mimic the short-term plasticity (STP) behavior of a spiking biological synapse.[10] When a sequence of voltage pulses is applied across the device, the current transmitted by the NOMFET is modulated depending on the frequency of the pulses and the past input activity of the device,[10,11] mimicking the facilitating or depressing behavior of a biological spiking synapse.[12] Research

on artificial synapse devices mimicking the plasticity of a biological synapse is a burgeoning field. Recently, Jo et al.[13] have observed STDP in Ag/Si-based memristor, Lai et al.[14] in polymer/Si nanowire transistor, Seo et al.[15] in oxide resistive memory, Kuzum et al. in phase-change memory.[16] Here, we demonstrate the STDP behavior of the NOMFET. First, we carefully analyze the behavior of this synapstor and show that it can be modelized by the memristor equations.[17,18] Thus, we follow the Linares-Barraco et al. suggestions[8,9] to successfully implement the STDP behavior with the NOMFET. Beyond the demonstration at a single device level, we also demonstrate that the NOMFET can be efficiently coupled with a CMOS platform emulating the pre- and postsynaptic neurons. Finally, we developed a behavioral macromodel suitable for device/circuit simulations using commercially available simulators (*Spectre-Cadence*).[19]

2. The Nanoparticle–Organic Memory Field-Effect Transistor: A Memristive Device

The NOMFET is based on a standard bottom gate/bottom source-drain organic transistor with gold nanoparticles (NPs) fixed at the gate dielectric/organic semiconductor (OSC) interface by surface chemistry (see the Experimental Section, and a previously reported detailed material characterization[10]). The STP behavior of the NOMFET is due to the internal charge/discharge dynamics of the NP/OSC system with typical time constants that can be adjusted between 1 to 10^2 s.[10] While we have demonstrated some simple neuroinspired plasticity for NOMFETs with a channel length L down to 200 nm, and NP diameter of 5 nm, working at a nominal bias of –3 V,[10] here for the sake of demonstration, all the experiments are reported for L = 5 µm NOMFETs and 20 nm diameter NPs working at a nominal voltage of –30 V, because these devices previously showed the largest plasticity amplitude (i.e., the largest modulation of the NOMFET output current, here analogous to the synaptic weight, by the applied spike sequence).[10] The channel width (W) is 1000 µm for the 5 µm length NOMFET, to maximize the output current, given the relative low mobility of the device (ca. 10^{-3} cm^2 V^{-1} s^{-1}).[10] Optimization of the OSC properties (not done here) will allow reaching a state-to-the art mobility of about 1 cm^2 V^{-1} s^{-1}, and will allow reducing the actual width by a factor 10^3. Further optimization would be the use of high-k dielectric to reach the same output current while downscaling W accordingly. Downscaling the NOMFET channel length to 30 nm (with 5 nm diameter NPs) is possible (we have already demonstrated a 30 nm channel length OFET[20]), but such a task would require a hard work for technological optimization, out of the scope of this proof of principle demonstration.

The NOMFET is used as a pseudo two-terminal device (**Figure 2**a): the drain (D) and gate (G) electrodes are connected together and used as the input terminal of the device, and the source (S) is used as the output terminal (virtually grounded through the ampmeter). To establish that it works as a memristive device, we write the output current - input voltage relation in the NOMFET according to the formalism proposed by Chua,[17] and we discuss the significance of the terms in this equation:

$$I_{DS}(t) = G(Q_{NP}(t),\, V_{DS}(t), t)\, V_{DS}(t) \quad (1)$$

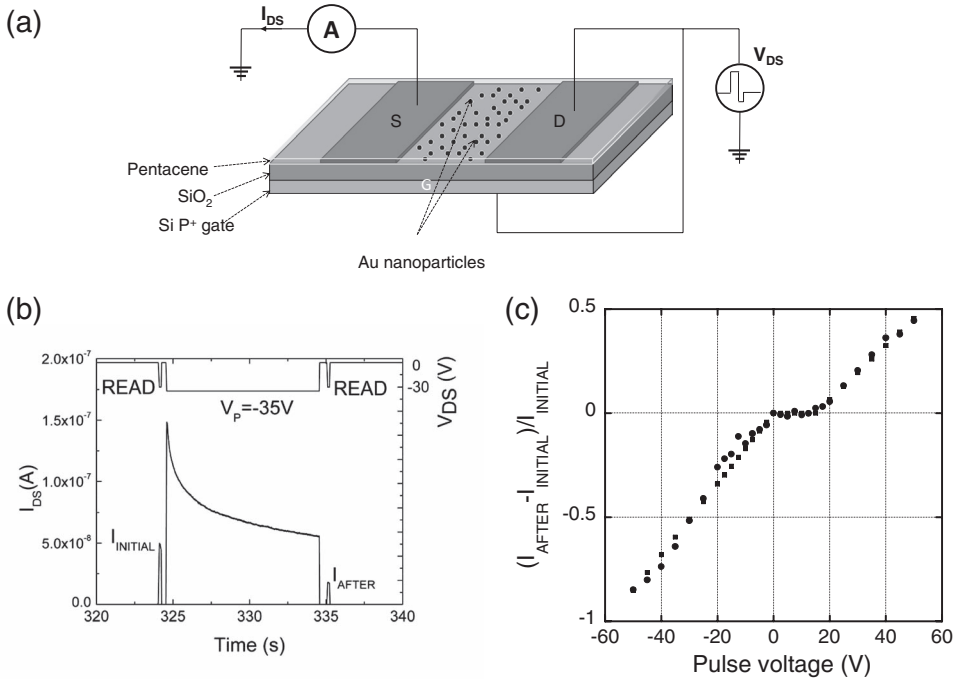

Figure 2. a) Schematic representation of the NOMFET and pseudo two-terminal connections of the device. b) Typical "single pulse measurement" used to characterized the NOMFET as a memristive device. The current is measured just before and after a large pulse of 10s in order to estimate the effect of the pulse voltage V_P on the NPs charge. c) Relative variation of the current as a function of the pulse voltage V_P. Dots are the experimental measurements and squares from the physical model (see the Supporting Information).

$$\dot{Q}_{NP}(t) = g(Q_{NP}(t), V_{DS}(t), t) \quad (2)$$

where G is the conductance of the device that includes the field effect, $V_{DS}(t)$ is the applied signal of time varying shape, and $Q_{NP}(t)$ the charges trapped in the NPs. For the NOMFET, $Q_{NP}(t)$ is the relevant internal parameter, and its first-order time derivative is given by the g function, which is the "memristive" function that describes how this internal parameter is updated as function of the internal state, the external voltage and time. A non-linear behavior of g is very interesting to implement synaptic plasticity and STDP.[6,8,9,18] A g function with a null value between negative and positive threshold voltages and increasing/decreasing parts above/below (respectively) these thresholds has been used to simulate STDP and learning capabilities in memristor-based neuroinspired circuits.[8,9]

To characterize the memristive behavior of the NOMFET, we measure the change of its internal parameter δQ_{NP} when voltage signal $V_{DS}(t)$ is a pulse of amplitude V_P and duration 10 s. This value of 10 s has been fixed in order to maximize the effect of the NP charge. This time is longer than the typical charging/discharging time constants (about 2–3 s)[10] for a NOMFET with a channel length of 5 µm and 20 nm NPs used for these experiments. Reducing the width of the charging pulse will give smaller variations of the current, but does not change the conclusions. The output current, before ($I_{initial}$) and after (I_{after}) the application of the charging pulse, are measured with a short read pulse (100 ms). This pulse is short enough to not modify the charge state of the NPs. Plotting $(I_{after}-I_{initial})/I_{initial}$, which is proportional to $\delta Q_{NP} = Q_{NP}^{after} - Q_{NP}^{initial}$ (Eq. S24, Supporting Information), versus V_P gives a representation of the g-function of the NOMFET. As the current at a given time t depends on the history of the device, we have developed a specific reset protocol (see Experimental Section, and Figure S1, Supporting Information) that sets the charge state of the NPs to the same $Q_{NP}^{initial}$ before each measurement at different V_P. Figure 2c shows the measured relative variation of the current (dots) as a function of V_P, i.e., the internal memristive-like function of the NOMFET. This function displays the three expected regions similarly to the resistance change in a voltage-controlled memristance:[8,9,17,18] i) For the negative voltage, the NPs are charged with holes, the Coulomb repulsion between the positively charged NPs and the OSC reduces the hole density in the conducting channel, the conductivity of the NOMFET is decreased. ii) For intermediate voltages ($V_{th1} < V < V_{th2}$), the effect of the input voltage on the charge state of the NPs is null. The charge state of the NPs cannot be changed. The physical meanings of the two threshold voltages, $V_{th1} \approx 0$ V and $V_{th2} \approx 15$ V, are discussed in the Supporting Information. iii) For large positive voltages, holes can be detrapped from the NPs, leading to a reverse effect, i.e., an increase in the conductivity of the NOMFET. The memristive g function shown in Figure 2c can be calculated using Equation S31 (Supporting Information) considering the three parts of the experimental curve. For simplicity, we assume the same time constants in Equation S31 ($\tau = \tau_0 = \tau_+ = \tau_- = 5$ s). This value is in good agreement with experimental values for the NOMFET.[10,11] The squares in Figure 2c are the fit of this model. Equation S31 gives two linear relationships for the two branches that fit relatively well our data.

3. Spike-Timing Dependent Plasticity Behavior of the Nanoparticle–Organic Memory Field-Effect Transistor

In a previous report,[10] the STP (short-term plasticity) is obtained by virtue of the unbalanced charging (during the application of a pulse at the input terminal) and discharging (between two successive pulses at the input terminal) behaviors of the NPs, respectively. Here, as detailed below, we play with the same charging/discharging dynamics to modulate (i.e., increase or decrease) the amount of charges trapped in the NPs when two pulses are now applied, one at the input and one at the output terminals of the NOMFET separated by a given time interval, leading to the long-term depression (LTD) or long-term potentiation (LTP) behavior of STDP, respectively. More precisely, **Figure 3**a shows the two different shapes of the spikes that are applied to the NOMFET, in agreement with the spike shape suggested previously[8] (Figure 1c). These spikes are designed so that – when applied alone – they do not induce any significant variation of conductivity. It means that NPs charging and discharging are well balanced between the negative and positive parts of the spike, respectively. The integral of the negative part of the signal ($V < V_{th1} \approx 0$ V) is equal to the integral of the positive part $V > V_{th2} \approx 15$ V), Figure 3a. To facilitate the measurement with the probe-station, the postsynaptic spike (that must be applied to the V_S terminal of the device) is inverted and applied to the V_D presynaptic terminal. Thus, the effective signal (Figure 3b) applied to the V_D terminal becomes equivalent to the application of the presynapse spike at the V_D terminal and the postsynapse spike at the V_S terminal (as a feedback). We check in section 4 that this procedure gives the same results as if we had applied the pre- and postsynaptic pulses directly to each of the two terminals. Note that the postsynaptic shape (Figure 3b) is slightly different from the presynaptic one to take into account the asymmetry of the memristive g function of the NOMFET (Figure 2c).

In a first stage, the presynapse spike is applied alone at the input terminal of the NOMFET. This step is crucial to verify that the presynapse spike alone does not change the conductivity of the NOMFET. In a second stage, we apply the pre- and postsynaptic spikes with a fixed time shift Δt between them (Figure 3b). The spikes have a frequency of 0.1 Hz and the conductivity of the NOMFET is read with a short pulse (100ms) synchronized with the spike sequence and applied 1s after the end of the pre-/postsynapse spike sequence (Figure 3b). The superposition of the pre- and postsynaptic spikes leads to an effective voltage across the NOMFET (bottom Figure 3b) in which the positive and negative contributions are no longer equal. This unbalanced contribution allows reproducing the basic principle of the STDP (Figure 3c). i) When the presynaptic neuron fires alone, the weight of the synapse is not changed. In the first part of Figure 3c (labeled "No postspike"), 10 presynaptic spikes are applied alone to the NOMFET. The conductivity of the NOMFET remains in its initial state. ii) When a presynaptic spike is correlated with a postsynaptic spike, the conductivity of the NOMFET is increased (Figure 3c labeled "With postspike", $\Delta t = +2$ s, 13 correlated spikes) due to the more important contribution of the positive part of the effective voltage across the NOMFET (i.e., the NPs are progressively discharged). The

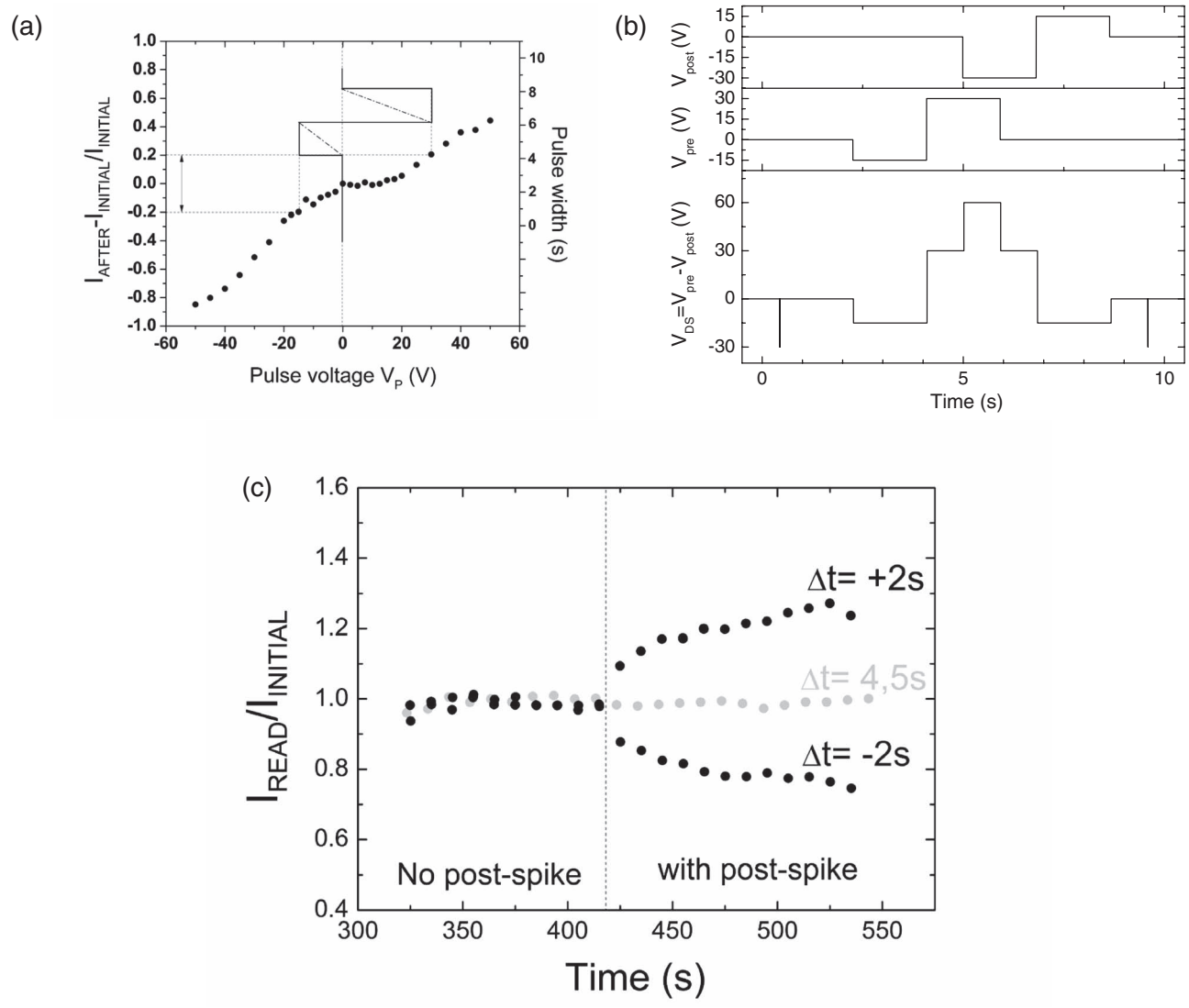

Figure 3. a) The two different pulses used to reproduce the STDP: square signal (solid lines), triangular signal (dash-dot line). In the case of the presynaptic pulse, the effect of the negative part, $V^- = -15$ V for 2 s, on the conductivity is equal to the effect of the positive part of the pulse, $V^+ = 30$ V for 2 s. b) Pre- and postsynaptic pulses superposition: the effective potential across the device is V_{PRE}- V_{POST} (in this case, Δt is 3 s). Note that the postsynaptic pulse is $V^- = -30$ V and $V^+ = 15$V to take into account the asymmetry of the memristive g function of the NOMFET. In this situation, the effect of the postsynaptic pulse alone on the conductivity is null. c) Typical STDP measurement. First, 10 presynaptic pulses are applied alone at 0,1 Hz in order to verify that the conductivity is not changed by the presynaptic signal alone. Next, 13 pre- and postsynaptic pulses are applied with 3 different Δt values.

synaptic weight is reinforced. iii) When the post- and presynaptic neuron spikes are anti-correlated ($\Delta t = -2$ s), the conductivity decreases, the contribution of the negative potential part dominates and the NPs are gradually more charged. The weight of the synapstor is depressed.

The same data are plotted as $\Delta I/I$ versus Δt curves (STDP learning curve) in **Figures 4**a and b for a sequence of 12 successive triangular and square spikes, respectively. Figure 4a (triangular spike) qualitatively looks like the one reported by Bi and Poo[4] for a biological synapse, by other groups with inorganic devices[13–16] and Linares-Barranco et al.[8,9] for simulations on memristors, i.e., a more or less sharp STDP function as shown in Figure 1c (right upper corner). Results in Figure 4b obtained with a rectangular spike show that the shape of the STDP learning window can be modulated successfully by changing the shape of the pulses, in good agreement with the behavior predicted by Linares-Barranco for a memristive device[8,9] (Figure 1c). Recent results on synapses based on phase change memory also showed experimentally that it is possible to change the shape of the STDP curves, albeit with a much more complicated sequence of spikes in this case.[16] Now, we obtain a more "squared" or "rounded" shape for the NOMFET STDP function, comparable with the simulation (right-lower corner in Figure 1c). Our model reproduces the experiments with a good qualitative agreement (squares Figure 4) considering five different values for the charge/discharge time constants depending on the voltage (Equation S32 and S34, Supporting Information). These time constants τ_i ($-2 < i < +2$, Equation S34)

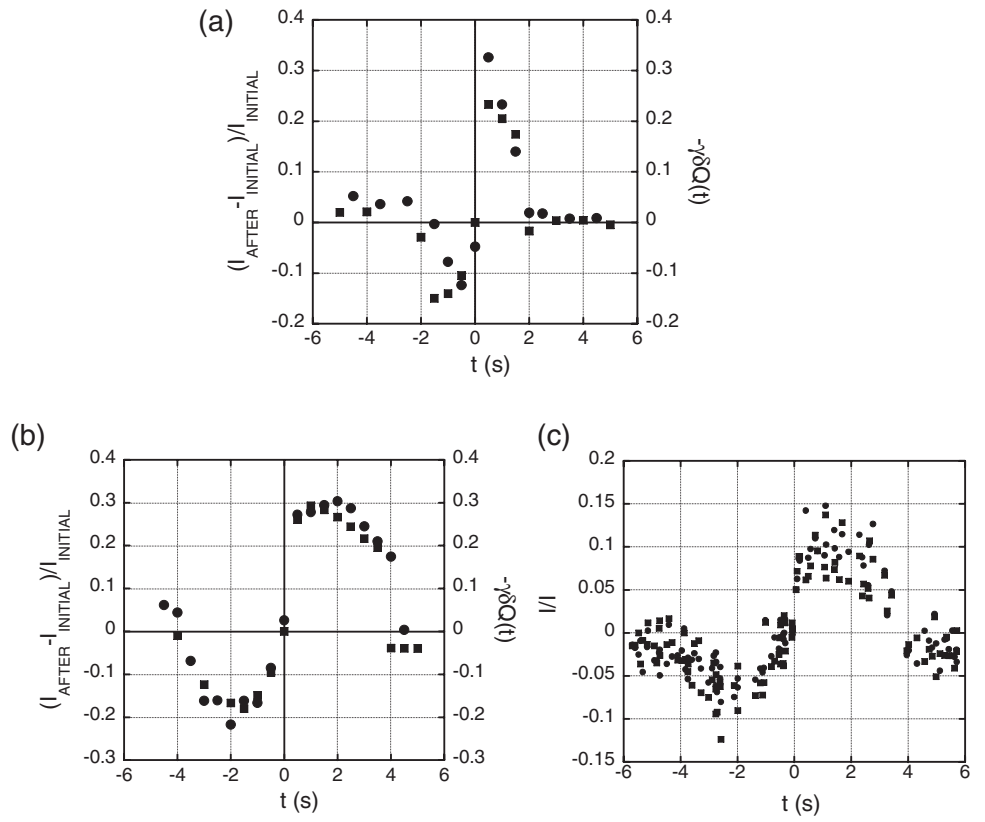

Figure 4. The relative variation of current is measured after 12 repetitions of the pre and post pulses pattern with a given Δt (as described in Figure 3b). The dots correspond to the experimental measurement $(I_{after} - I_{initial})/I_{initial}$ and the squares are the model calculation $-\gamma\delta Q_{NP}$ (see the Supporting Information). a) STDP function obtained with the triangle-shape pulses. b) STDP function obtained with the square-shape pulses. c) STDP learning function acquired with the electronic-board for two NOMFETs (dots and squares) measured simultaneously.

are in the range 0.3 to 5 s, in good agreement with previous measurements showing that the charging/discharging of the NPs follows a multi-time constant dynamics in this time-scale range (Figure S5 in the Supporting Information in Ref. [10]). Finally, we can note that the approximation used in Eq. S24 ($\gamma\delta Q_{NP} << 1$) is justified (see Figure 2c) at low bias and is reasonable for bias voltages in the range ± 30V used in the STDP experiments. Nevertheless, the model-experiment agreement seems not strongly affected when $\gamma\delta Q_{NP}$ approaches 1 at higher voltages. Finally, we note that the STDP amplitude (from –15% to 30%, Figure 4) is lower than for biological synapse (–40 to 100%) as reported by Bi and Poo,[4] however, our results are larger or similar to the ones reported by other groups.[13–16] We expect that these performances can be improved by a careful technology optimization, for instance, recent STDP results with phase change memory (PCM)[16] – a much more mature technology – reached a dynamic between –40 and 110%.

4. Hybrid Nanoparticle–Organic Memory Field-Effect Transistor/Complementary Metal Oxide Semiconductor System

Instead of using a single device connected to a probe-station, a more realistic demonstration of the STDP behavior of the NOMFET is obtained by interfacing these synapstors with a CMOS-based electronic board to emulate the neurons and generate pre- and postsynaptic spikes, which are now directly applied to the input and output of several NOMFETs. Several NOMFETs were mounted in a TO case and plugged on the electronic board (see Figure S2, Supporting Information). This board is driven by an FPGA and is remotely controlled by a PC (see details in the Supporting Information). Series of rectangular spikes, identical to those used for the previous measurements, are applied simultaneously to two NOMFETs, with a randomly generated time interval Δt between the pre- and postsynaptic spikes. The output currents of these NOMFETs are acquired with the electronic-board (see Figure S2, Supporting Information). The $\Delta I/I$ versus Δt measured simultaneously for two NOMFETs are shown in Figure 4c. The STDP function obtained with this NOMFET/CMOS system is in good agreement with the one measured point-by-point for a NOMFET connected with the probe-station as shown in Figure 4b. In addition this is, to the authors' best knowledge, the first actual implementation of STDP on a dynamic device that meets the following conditions: i) The correct behavior is achieved regardless of the initial state of the device, as the timing between the pre- and postsynaptic spikes is random between each measurement (the same STDP behavior, Figure 4c, has been obtained here with random Δt, while the data shown in Figures 4a and 4b have

been recorded for a linear sequence of Δt from –5 to +5 s). ii) The behavior remains consistent and very well reproducible regardless of the characteristics of the devices. Indeed, there is a factor 10 in the mean conductivity ratio between the two NOMFETs used in Figure 4c and yet the relative change in conductivity is the same for the two devices, i.e., the variability on the dynamical behavior of the NOMEFT is very low. This behavior is due to the fact that the STDP is based on a temporal coding, and only the relative variation of the NOMFET conductivity obtained through the applied pulses, and the natural relaxation of the NPs, impose the dynamics. This means that with STDP, we have a reliable way of programming conductivity changes using temporal information coding with seemingly unreliable devices. As a consequence, STDP and NOMFET can be useful to implement some learning algorithms in neural network circuits without to pay too much attention to some common variability sources, such as physical dimensions, reproducibility and control of the technological steps.

5. Behavioral Macromodel for Neuroinspired Circuit Simulation

The physical model developed for such a diode-connected NOMFET (**Figure 5**a) is implemented in *Spectre-Cadence*[19] for simulating neuroinspired circuits using STDP and NOMFET. The NOMFET device can be described behaviorally using the macro model circuit shown in Figure 5b. The terminal drain and source voltage V_D and V_S are copied to an internal diode in series with a resistor, attenuated by a scaling factor α. This is to adapt the operating voltage (few tens of volts) of the NOMFET to a regular silicon diode used in CADENCE. The current through the diode i_{ds0} is sensed and copied to the bottom input of element $m()$. Element $m()$ computes the following function:

$$m(i_{ds0}, w) = Ai_{ds0}e^{-w/w_0} \quad (3)$$

where w is a circuit variable (a voltage) that describes the evolution of the charge in the NPs, $w(t)$ is proportional to $\delta Q_{NP}(t)$ (Equation S36 in the Supporting Information). Internal voltage w is generated by feeding a resistor R and a capacitor C with a current source of value $-C\rho(V_{DS})$. The time constant in eqs. (S35–S39) is such that $\tau = RC$. This way this circuit implements Equation S38. This macromodel is used to simulate the behavior of the NOMFET when stimulated by a signal such as the one shown in Figure 2b, a pulse $V_P = -35$ V during 10s. By holding $V_S = 0$ and applying a negative –35 V pulse during 10 s at V_D, we obtain the signal evolutions shown in Figure 5c. The different parameters were optimized to best fit the measured I_{DS} signal in Figure 2b: $\tau = 2.2$ s ($C = 1$ F, $R = 2.2\ \Omega$), $A = 10^{-6}$, R_d the diode resistance = 20 kΩ, $V_{th} = 15$V, $w_0 = 0.16$V and $\alpha = 0.1$. The internal diode is described by $i_{ds0} = I_{d0}e^{V_{diode}/U_T}$ where $U_T = kT/q$ is the thermal voltage (≈ 26mV) and $I_{d0} = 8 \times 10^{-20}$ A. Simulated results in Figure 5c are in very good agreement with the experiments (Figure 2b). Again, note that the fitted time constant is in good agreement with experimental values for the NOMFET as reported elsewhere.[10] These results validate the macromodel that can be further used to simulate neuroinspired circuits using STDP learning rules.

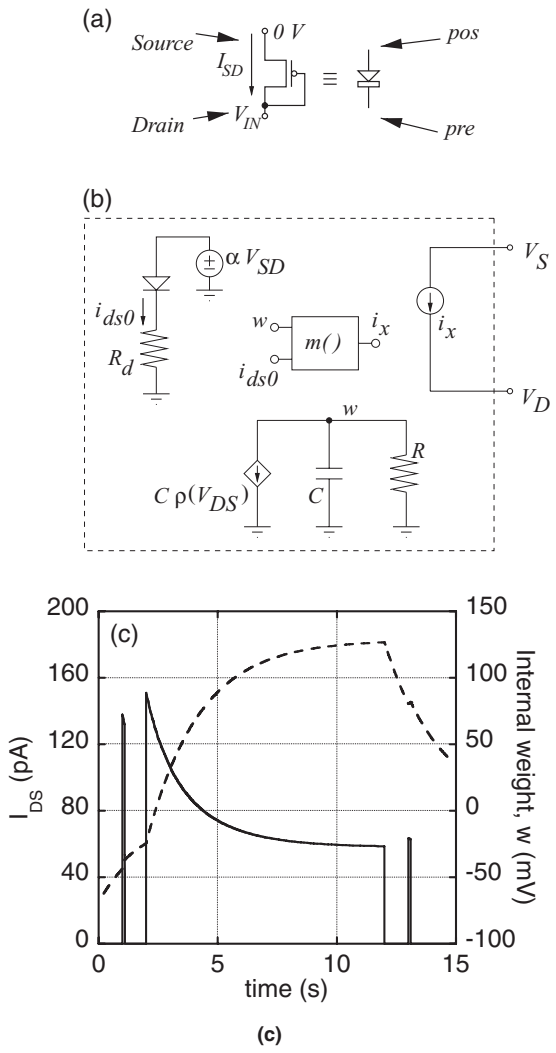

Figure 5. a) The NOMFET is a p-type FET, it is used in a diode-like connected configuration. Source S is the top terminal, drain D is the bottom terminal. I_{DS} is either zero or positive. It is equivalent to a diode. When used as an STDP synapse (see Figure 2a), bottom terminal is the presynaptic connection and top terminal is the postsynaptic connection. b) NOMFET macromodel implemented in *Spectre-Cadence*.[19] c) Simulation of the NOMFET with the macromodel: output current (solid line, left scale) and evolution of the internal weight parameter w (dashed line, right scale).

6. Discussion and Conclusion

Finally, we can notice that the potentiation (depression) reported here for the correlated (anticorrelated) spikes resembles that of a biological synapse (albeit with spike signals adapted to the NOMFET for which the physical mechanisms responsible for the STDP behavior are clearly different from the ones in a biological synapse) as reported by Markram et al.[3] and by Bi and Poo,[4] while at different time scales due to the different internal dynamics of the two systems. We have already demonstrated that NOMFET with a smallest channel length (L = 200 nm, and 5 nm NPs), working at a lower voltage (–3 V) exhibit neuroinspired short-term plasticity (STP) with smaller time constants (~1 s, see Figure 6c in Ref. [10]), while with a

weaker amplitude.[10] So we believe there is room to improve the neuroinspired behavior of these synapstors and their future use in neuroinspired computing circuits and architectures. For instance, the actual low time scale response of NOMFET can be ascribed to two features. i) The fist one is the low charge/discharge time constants of the NPs, which are capped by alkyl chains (see the Experimental Section) acting as tunnel barrier. ii) The relatively low mobility of charges in the pentacene/NP channel,[10] which reduces the functioning speed of the device. Improvements (i.e., shorter time-scale, closer to the one of a biological synapse) can probably be attainable by changing the nature of the NP capping molecules (e.g., using more conducting π-conjugated molecules), and/or optimizing the deposition/nature of the organic semiconductor to increase the charge-carrier mobility.

7. Experimental Section

Device Fabrication: The synapstors are made on a highly doped (~10^{-3} Ω.cm) p-type silicon covered with a thermally grown 200 nm thick silicon dioxide. After a usual wafer cleaning (sonication in chloroform for 5 min, piranha solution (H_2SO_4/H_2O_2, 2/1 v/v) for 15 min – *caution: the preparation of the piranha solution is highly exothermic and reacts violently with organics*, ultraviolet ozone cleaning (ozonolysis) for 30 min), we evaporated titanium/gold (20/200 nm) electrodes, patterned by optical lithography and lift-off. To attach the NPs, the gold (Au) electrodes were functionalized with a 2-amino ethanethiol molecules (10 mg mL^{-1} in ethanol) during 5 h. After rinse (isopropanol) and subsequent drying in argon stream, the SiO_2 surface was functionalized at 60 °C during 4 min by 3-aminopropyl trimethoxysilane (APTMS) molecules (from ABCR) at 1.25 µL mL^{-1} (in anhydrous toluene).[21] The reaction took place in a glove-box (MBRAUN) filled with nitrogen (less than 1 ppm of oxygen and water vapor). We removed non-reacted molecules by rinse in toluene, and then in isopropanol under sonication, and the samples were dried under argon stream. This sample was then dipped in an aqueous solution of citrate-stabilized Au-NP (colloidal solution purchased from Sigma–Aldrich, 20 ± 3 nm in diameter) overnight under argon atmosphere, followed by cleaning with deionized water and isopropanol, and drying under argon stream. NP concentration in the solution and duration of the reaction are selected from our previous work to have a NP density on the surface of about 10^{11} NP cm^{-2} that gives the best results for the synaptic behavior of the NOMFET.[10] Then, the Au-NPs were encapsulated by dipping in a solution of 1,8-octanedithiol (from Aldrich) in ethanol (10 µL mL^{-1}) during 5h. The sample was finally rinsed in alcohol and dried in argon stream. The device is completed by evaporating (substrate kept at room temperature during the evaporation) 35 to 50 nm thick of pentacene at a rate of 0.1 Å s^{-1} More details on the structural characterizations of the NPs networks and pentacene films (SEM, AFM,…) have been provided previously.[10]

Electrical Measurements: The NOMFET were contacted with a micromanipulator probe station (Suss Microtec PM-5) inside a glove box (MBRAUN) with controlled nitrogen ambient (less than 1 ppm of water vapor and oxygen). Such a dry and clean atmosphere is required to avoid any degradation of the organics. The input spikes were delivered by an arbitrary waveform generator (Tabor Electronics 5062) remote controlled by a PC. The pulse and spike sequences were designed with Matlab. The output currents were measured with an Agilent 4155C semiconductor parameter analyzer.

Reset Potocol: The reset signal is based on the same principle than the one used to remove the permanent magnetization of a magnet. We impose a decreasing sinusoidal input voltage (see Figure S1, Supporting Information) with a large period and a large initial voltage (the period and initial voltage must be large enough in comparison to the input voltage used during the operation/characterization of the device). The NPs are alternatively charged and discharged with a decreasing magnitude. Even if this initial state of charge of the NPs is different from the virgin state of charge of the NPs (i.e.,in the as-deposited state), it allows starting a specific measurement from the same initial condition.

Supporting Information

Supporting Information is available from the Wiley Online Library or from the author.

Acknowledgements

This work was funded by the European Union through the FP7 Project NABAB (Contract FP7-216777). We thank D. Guérin, K. Lmimouni, S. Lenfant (CNRS-IEMN) for help and advises during the device fabrication, and D. Querlioz (CNRS-IEF) for helpful discussions.

Received: August 17, 2011
Revised: October 24, 2011
Published online: December 13, 2011

[1] D. Hebb, *The Organization of Behavior*, Wiley, New York **1949**.
[2] K. Gant, C. Bell, V. Han, *J. Physiol. Paris* **1996**, *90*, 233.
[3] H. Markram, J. Lubke, M. Frotscher, B. Sakmann, *Science* **1997**, *275*, 213.
[4] G. Q. Bi, M. M. Poo, *J. Neurosci.* **1998**, *18*, 10464.
[5] J. Sjöström, W. Gerstner, *Scholarpedia* **2010**, *5*, 1362.
[6] G. S. Snider, *Proc. IEEE ACM Int. Symp. Nanoscale Architectures* **2008**, 85.
[7] D. B. Strukov, G. S. Snider, D. R. Stewart, R. S. Williams, *Nature* **2008**, *453*, 80.
[8] B. Linares-Barranco, T. Serrano-Gotarredona, *Proc. 9th IEEE Conf. Nanotechnol.* **2009**, 601.
[9] C. Zamarreno-Ramos, L. Camuñas-Mesa, T. Serrano-Gotarredona, B. Linares-Barranco, *Front. Neurosci.* **2011**, **5**, 26.
[10] F. Alibart, S. Pleutin, D. Guérin, C. Novembre, S. Lenfant, K. Lmimouni, C. Gamrat, D. Vuillaume, *Adv. Funct. Mater.* **2010**, *20*, 330.
[11] O. Bichler, W. Zhao, F. Alibart, S. Pleutin, D. Vuillaume, C. Gamrat, *IEEE Trans. Electron Devices* **2010**, *57*, 3115.
[12] J. A. Varela, K. Sen, J. Gibson, J. Fost, L. F. Abbott, S. B. Nelson, *J. Neurosci.* **1997**, *17*, 7926.
[13] S. H. Jo, T. Chang, I. Ebong, B. B. Bhadviya, P. Mazumder, W. Lu, *Nano Lett.* **2010**, *10*, 1297.
[14] Q. Lai, L. Zhang, Z. Li, W. F. Stickle, R. S. Williams, Y. Chen, *Adv. Mater.* **2010**, *22*, 2448.
[15] K. Seo, I. Kim, S. Jung, M. Jo, S. Park, J. Park, J. Shin, K. P. Biju, J. Kong, K. Lee, B. Lee, H. Hwang, *Nanotechnology* **2011**, *22*, 254023.
[16] D. Kuzum, R. G. D. Jeyasingh, B. Lee, H.-S. P. Wong, *Nano Lett.* **2011**, DOI:10.1021/nl201040y.
[17] L. O. Chua, *IEEE Trans. Circuit Theory* **1971**, *18*, 507.
[18] M. Di Ventra, Y. V. Pershin, L. O. Chua, *Proc. IEEE* **2009**, *97*, 1717.
[19] Cadence Virtuoso platfom with Spectre simulator. Cadence Design Systems, Inc. www.cadence.com.
[20] J. Collet, O. Tharaud, A. Chapoton, D. Vuillaume, *Appl. Phys. Lett.* **2000**, *76*, 1941.
[21] D. F. Siqueira Petri, G. Wenz, P. Schunk, T. Schimmel, *Langmuir* **1999**, *15*, 4520.